NJC

ROYAL SOCIETY OF CHEMISTRY

PAPER

View Article Online
View Journal

Cite this: DOI: 10.1039/d0nj02785e

Doxorubicin-loaded micelles with high drug-loading capacity and stability based on zwitterionic oligopeptides†

Weili Xue, * Ashish Trital, Sihang Liu and Liangbo Xu

To simplify the preparation process and increase the drug-loading capacity of antitumor nanodrugs, doxorubicin-loaded micelles based on zwitterionic oligopeptides were fabricated through two step reactions in mild conditions. Zwitterionic oligopeptides Glu–Lys–Cys–Glu–Lys (EKCEK) were reacted with methacrylohydrazide (MAH) by click reaction, the product was further conjugated with doxorubicin (Dox) to form amphipathic molecules, and finally the amphipathic molecules self-assembled into doxorubicin-loaded micelles (EKCEK–Dox) in deionized water. TEM and DLS results showed that the EKCEK–Dox micelles were of the regular sphere, with the mean diameter approximately 70 nm. The drug-loading capacity of the prepared micelles was up to 44.6%, and the micelles were very stable in PBS solution. *In vitro* antitumor experiment showed that the EKCEK–Dox micelles had significant inhibition efficacy on MCF-7 cells, which was much better than the clinical antitumor drug (Doxil®). The IC50 of the EKCEK–Dox micelles (5.6 μg Dox equiv. per mL) was significantly lower than Doxil (8.9 μg Dox equiv. per mL). Therefore, the drug delivery system based on zwitterionic oligopeptides will be a promising strategy for cancer chemotherapy.

Received 2nd June 2020,
Accepted 7th July 2020

DOI: 10.1039/d0nj02785e

rsc.li/njc

Introduction

In recent years, anticancer nanodrugs provide a better treatment strategy for human malignancies.[1–4] Liposomal doxorubicin-Doxil® is the first clinically approved nanodrug for treating various cancers, including ovarian cancer, multiple myeloma, Kaposi's sarcoma and metastatic breast cancer.[5,6] The success of liposomal doxorubicin can be ascribed to the following reasons. Firstly, the amount of loaded doxorubicin (Dox) is significantly increased through the pH-gradient preparation method. What's more, the drug-loaded system can be transmitted in blood circulation by stealth after the surface of the drug carrier is PEGylated. Compared with free Dox, liposomal doxorubicin can efficiently prolong circulation time, improve biodistribution and therapeutic effect and reduce cardiotoxicity.[7–9] However, liposomal doxorubicin still has its deficiencies such as poor tumor selectivity and severe side effects like foot and mouth disease and stomatitis.[10] Although PEGylated drug carriers have broad prospects and significant advantages, only very few nanodrugs are used in the clinic. Moreover, anticancer nanodrugs already used in the clinic, including liposomal doxorubicin, merely slightly increased the survival rate of the patients.[11–15]

Polymeric vesicles are a kind of very stable carrier, which are constructed from the self-assembly of amphiphilic block copolymers.[16–19] Compared with liposome, apart from stronger stability, the surface of polymeric vesicles can be modified functionally, which makes polymeric vesicles increasingly attractive.[20–23] Therefore, many researchers have designed various polymeric vesicles response to stimulus signals such as pH, temperature, redox potentials, enzyme and magnetic field.[24–31] Moreover, researchers have developed some polymeric vesicles with tumor-targeting function by modifying the surface of polymeric vesicles with peptide, human serum albumin, antibody, folate and hyaluronic acid.[32–35] In addition to various signal response and tumor-targeting functions, the stability of a drug carrier in blood circulation is the prerequisite for delivering the drugs to the tumor site. Zwitterionic materials attract researchers' attention due to its excellent *anti*-nonspecific protein absorption property, which makes zwitterionic materials become promising drug-loaded materials.[36–38] Uniform charge distribution, low net charge density and strong hydratability are the internal reasons for the non-fouling capacity of zwitterionic materials.[39]

Despite a large number of intricately designed drug delivery systems have been reported, it is the fact that only a few anticancer nanodrugs are approved for the clinic. Besides ensuring

Key Laboratory of Biomass Chemical Engineering of Ministry of Education, College of Chemical and Biological Engineering, Zhejiang University, Hangzhou, Zhejiang 310027, China. E-mail: xueweili1028@zju.edu.cn

† Electronic supplementary information (ESI) available. See DOI: 10.1039/d0nj02785e

Scheme 1 Illustration of preparing the EKCEK–Dox micelles.

therapeutic effect and safety, the complexity of preparation method and the cost also play a vital role in the transformation of nanodrugs into clinical antitumor medicines. For promoting the development of anticancer nanodrugs, the novel doxorubicin-loaded micelles based on Glu–Lys–Cys–Glu–Lys (EKCEK) were introduced in this study (Scheme 1). The micelles were equipped with stealth function under the protection of hydrophilic EKCEK shells. In addition, EKCEK conjugated with Dox through hydrazone bond, which could be hydrolyzed in low pH conditions and then released the loaded drugs quickly. More importantly, the molecular weight of EKCEK is close to Dox molecules so that the drug-loading capacity of the final product is very high. Therefore, the doxorubicin-loaded micelles based on EKCEK will be an excellent candidate for future antitumor nanodrugs.

Results and discussion

Synthesis of MAH and EKCEK–MAH

Before preparing the drug-loaded micelles based on zwitterionic oligopeptides, MAH was synthesized, which acted as a bridge connecting Dox and EKCEK. After that, EKCEK reacted with MAH to form a drug-loading precursor EKCEK–MAH through Michael addition reaction. ^{1}H NMR spectra of synthesized MAH and EKCEK–MAH were shown as Fig. S1 and S2 (ESI†).

Particle size and zeta potential characterization of EKCEK–Dox micelles

The morphology of drug-loaded micelles was characterized by transmission electron microscopy (TEM). As shown in Fig. 1a, the prepared micelles were of a regular sphere, and particle sizes of the micelles were around 50–100 nm, which was beneficial for blood circulation and enhanced penetration and retention (EPR) effect. Fig. 1b showed the partially enlarged image of the drug-loaded micelles and the particle size was uniform. It was shown that the center color of the micelles was dark, whereas the edge color was light, which demonstrated that hydrophobic Dox molecules were successfully encapsulated by the hydrophilic EKCEK shell. Particle size distribution measured by DLS was shown as Fig. 1c, and it suggested the particle size of the most drug-loaded micelles was at the range of 60–80 nm, which was consistent to the results shown by TEM. Zeta potentials of EKCEK–Dox at different pH values (pH 5–8) were characterized and the results were shown as Fig. 1d. At pH 5.6–8, the surface of EKCEK–Dox was negatively charged, and only when the pH was below 5.5, the surface of EKCEK–Dox had a slightly positive charge.

Stability of EKCEK–Dox micelles

Stability of the EKCEK–Dox micelles was characterized by measuring the particle size variation of the drug-loaded

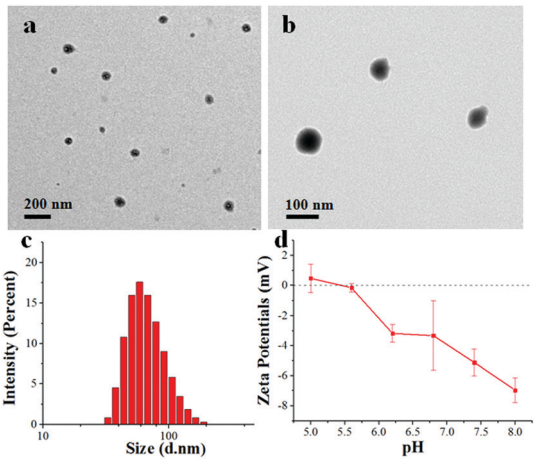

Fig. 1 Morphology characterization, particle size distribution and zeta potentials of the drug-loaded micelles prepared by EKCEK oligopeptides (a) TEM image of the drug-loaded micelles, (b) partially enlarged TEM image of the drug-loaded micelles, (c) size distribution of the drug-loaded micelles measured by DLS, (d) zeta potentials of the drug-loaded micelles at different pH values. Data are presented as mean ± SD (n = 3).

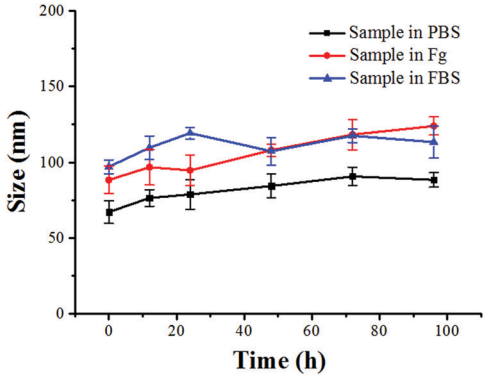

Fig. 2 Particle size variation of EKCEK–Dox dissolved in PBS, 100% FBS and 3 mg mL^{-1} Fg in PBS at 37 °C.

micelles dissolved in PBS, 100% FBS and 3 mg mL^{-1} bovine fibrinogen (Fg) in PBS within 96 h. As shown in Fig. 2, the particle size of EKCEK–Dox in PBS was smallest and always stayed around 50–80 nm within 96 h. When dissolved 3 mg mL^{-1} Fg in PBS, the particle size of the EKCEK–Dox micelles increased slightly, and the particle size of the micelles always stayed below 120 nm. Similarly, the stability of EKCEK–Dox in 100% FBS was still very high, and the particle size fluctuated between 100 nm and 120 nm. The increase of particles size should be due to the presence of protein molecules in a complex medium. In short, the drug-loaded micelles can keep stable in different protein solutions, which will benefit to the safe transportation of the micelles in blood circulation.

Drug-loading capacity and *in vitro* drug release of the EKCEK–Dox micelles

EKCEK–MAH conjugated with Dox by hydrazone bond and self-assembled into stable drug-loaded micelles in which Dox formed a hydrophobic core and EKCEK formed a hydrophilic

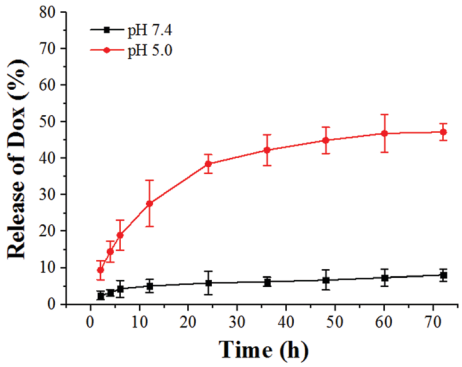

Fig. 3 *In vitro* drug release profiles of the drug-loaded micelles dissolved in pH 5.0 and 7.4 NaAc buffers respectively.

shell. According to the molecular weight of the final compound EKCEK–Dox, theoretical drug-loading capacity was 44.16% and the actually measured value was 44.6%. Because the hydrazone bond can be hydrolyzed in acidic conditions, drug release of EKCEK–Dox would be influenced by ambient pH conditions. Therefore, the cumulative drug release of EKCEK–Dox dissolved in pH 5.0 and 7.4 NaAc buffer was measured, and the result was shown as Fig. 3.

In pH 7.4 conditions, the cumulative drug release of EKCEK–Dox was always below 10% within 72 h, which demonstrated that the drug-loaded micelles were very stable, and drug leakage of EKCEK–Dox in physiological pH conditions was very low. For that reason, the drug-loaded system can be circulated in the blood safely. Compared with physiological pH conditions, the cumulative drug release of EKCEK–Dox increased remarkably when pH decreased to be 5.0, and nearly 40% of the drugs were released in the first 24 h. After that, the drug release of EKCEK–Dox increased slowly over time, and the total drug release was close to 50% within 72 h.

In vitro inhibition efficacy of the EKCEK–Dox micelles on MCF-7 cells

The *in vitro* inhibition efficacy of the EKCEK–Dox micelles on MCF-7 cells was evaluated by MTT assay, and the results were shown as Fig. 4. Free Dox showed the highest inhibition efficacy on MCF-7 cells, and the cell viability decreased dramatically with the concentration of Dox increasing. The IC50 of free Dox was 4.8 μg mL^{-1}, and almost all MCF-7 cells were killed when the concentration of Dox reached 20 μg mL^{-1}. By contrast, the *in vitro* inhibition efficacy of the EKCEK–Dox micelles was similar to free Dox, and much better than Doxil. The IC50 of EKCEK–Dox was 5.6 μg Dox equiv. per mL, which was significantly lower than Doxil (8.9 μg Dox equiv. per mL).

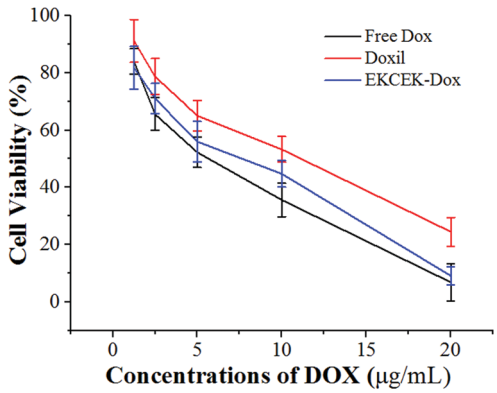

Fig. 4 *In vitro* inhibition efficacy of free Dox, Doxil and EKCEK–Dox on MCF-7 cells.

It is well known that free Dox is a small molecule so that it can quickly diffuse into the tumor cells and kill them. Therefore, it is understandable that free Dox has the highest inhibition efficacy among the three groups. Doxil is a kind of nanodrug coated with the polyethylene glycol (PEG) layer, which will impair the internalization of Doxil by tumor cells.[40] That may be the main reason why the inhibition efficacy of Doxil on MCF-7 cells is the lowest among the three groups. With respect to EKCEK–Dox, high drug-loading capacity might promote the cellular internalization of the micelles by tumor cells. Therefore, the cellular uptake behavior and mechanism of the EKCEK–Dox micelles by MCF-7 cells were further investigated.

Cellular uptake of the EKCEK–Dox micelles by MCF-7 cells

Hoechst 33 342 was used to stain the nuclei of MCF-7 cells so that whether Dox molecules entered the nucleus or not could be observed by an inverted fluorescence microscope. Fluorescence images of MCF-7 cells incubated with the micelles were shown as Fig. 5.

At 2 h, all red fluorescence of Dox in three groups was not obvious, which demonstrated that the amount of drugs endocytosed by MCF-7 cells was low within 2 h. Among the three groups, the intensity of red fluorescence of Doxil group was the lowest, and the merged image indicated almost no Dox molecules entered the nuclei. Dox fluorescence brightness of EKCEK–Dox and free Dox groups was similar, indicating the internalization capacity of EKCEK–Dox was comparable to free Dox, much better than Doxil. In addition, free Dox is small molecule so that it can be cleared quickly in blood circulation, whereas the EKCEK–Dox micelles can accumulate in tumor site through EPR effect. At 4 h, the difference between EKCEK–Dox and Doxil was widened. The Dox fluorescence of MCF-7 cells incubated with EKCEK–Dox was much brighter than incubated with Doxil, suggesting the internalization process of EKCEK–Dox by MCF-7 cells was accelerated over time, whereas the internalization process of Doxil by MCF-7 cells was still very slow. The difference of cellular internalization rate between EKCEK–Dox and Doxil also demonstrated zwitterionic shell was more beneficial for the internalization of nanodrugs by tumor cells than the PEGylated one.

To sum up, free Dox was the fastest to be endocytosed by MCF-7 cells and diffuse into the nuclei. Although endocytosis rate of EKCEK–Dox was similar to free Dox, EKCEK–Dox failed to deliver more Dox molecules into the nuclei. It can be speculated that in the presence of a super-hydrophobic core, the hydrazone bond cannot be hydrolyzed rapidly enough to release Dox molecules so that there were not so much Dox molecules in the nuclei within 4 h.

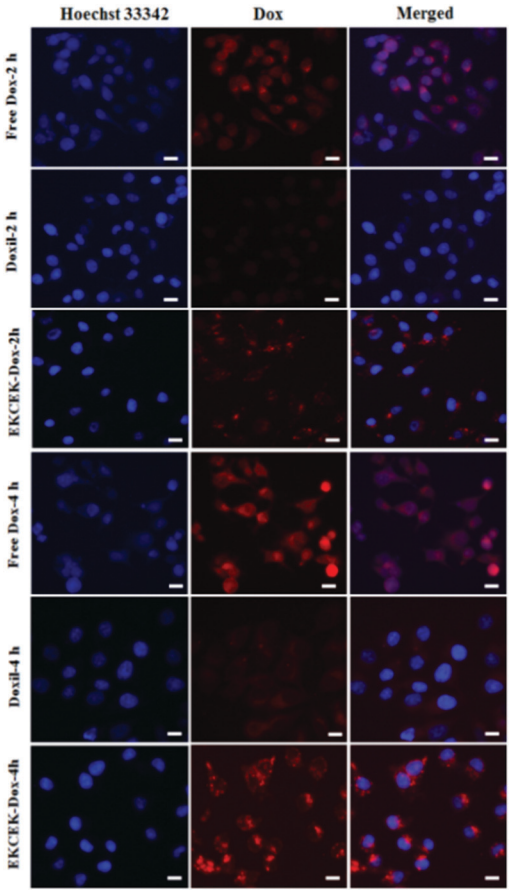

Fig. 5 Fluorescence images of MCF-7 cells incubated with free Dox, Doxil and EKCEK–Dox for 2 h and 4 h respectively (red represents natural fluorescence color of Dox molecule; blue represents Hoechst 33 342 which was used to stain cell nuclei. Scale bar represents 20 μm).

Endocytosis pathway of the EKCEK–Dox micelles by MCF-7 cells

The EKCEK–Dox micelles was co-incubated with MCF-7 cells intervened with different kinds of endocytosis inhibitors for 4 h, and then the endocytosis pathway of EKCEK–Dox by MCF-7 cells was analyzed through flow cytometry (FCM) measurement. As shown in Fig. 6, the red curve represented the result of a positive control group in which no any endocytosis inhibitor was added, and only EKCEK–Dox was co-incubated with MCF-7 cells. Therefore, the endocytosis amount of EKCEK–Dox by MCF-7 cells was set as 100%. Orange, green and blue curves represented FCM results of MCF-7 cells intervened with genistein, chlorpromazine hydrochloride and amiloride hydrochloride respectively. The results suggested that genistein and amiloride hydrochloride had few influences on cellular uptake of EKCEK–Dox by MCF-7 cells in comparison to the positive control group. The green curve suggested that Dox fluorescence intensity of MCF-7 cells intervened with chlorpromazine hydrochloride decreased dramatically, proving cellular internalization of the EKCEK–Dox micelles by MCF-7 cells were mostly inhibited by chlorpromazine hydrochloride. Therefore, it could be concluded that the endocytosis pathway of the EKCEK–Dox micelles by MCF-7 cells was clathrin-dependent.

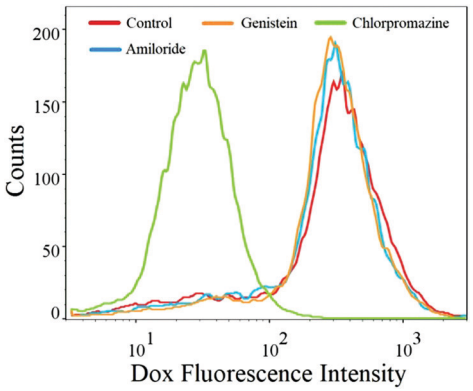

Fig. 6 Flow cytometry studies of MCF-7 cells following 4 h incubation with the EKCEK–Dox micelles in the presence of cellular uptake inhibitors like chlorpromazine, amiloride and genistein.

Experimental

Materials

Glu–Lys–Cys–Glu–Lys (EKCEK) (purity 99.98%) oligopeptides were purchased from GL Biochem (Shanghai) Co., Ltd. Methacryloyl chloride and *tert*-butyl carbazate (98 wt%) were purchased from Aladdin-reagent (Shanghai, China) Co., Ltd. Doxorubicin hydrochloride (Dox·HCl) was purchased from Zhejiang Haizheng pharmaceutical Co., Ltd. Sodium acetate (NaAc), acetic acid (AcOH), anhydrous methanol, anhydrous sodium sulfate, anhydrous tetrahydrofuran (THF) and triethylamine (TEA) were purchased from Sinoreagent (Shanghai, China). All buffers used in this study were filtrated through a 0.45 μm filter before use. Human breast cancer cells (MCF-7) were obtained from Shanghai academy of life sciences, Chinese academy of sciences.

Synthesis of methacrylohydrazide hydrobromide (MAH·HBr)

MAH·HBr was synthesized through two-step reactions, and the synthesis procedure was shown in Fig. S3 (ESI†). Concrete operations should refer to ESI.†

Preparation of drug-loaded micelles based on EKCEK

Synthesis route of the drug-loaded micelles based on EKCEK was shown as Scheme 2. Concrete operations should refer to ESI.†

Particle size and zeta potential characterization of the EKCEK–Dox micelles

The EKCEK–Dox micelles dissolved in deionized water were used for TEM characterization. The particle size of EKCEK–Dox dissolved in PBS was measured by dynamic light scattering (DLS). Zeta potentials of EKCEK–Dox dissolved in McIlvaine Buffer with different pH were checked by Malvern Zetasizer ZS (Malvern Instruments, UK). The concentration of all samples used in the above characterization was 0.2 mg mL^{-1}.

Stability measurement of the EKCEK–Dox micelles

The stability of the EKCEK–Dox micelles was evaluated by monitoring the particle size variation of the micelles in different kinds of protein-contained solutions through DLS.

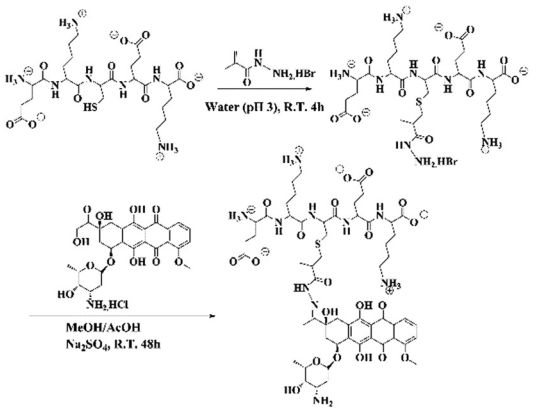

Scheme 2 Synthesis route of drug-loaded micelles based on EKCEK.

EKCEK–Dox lyophilized powders were respectively dissolved in PBS, 100% fetal bovine serum (FBS) and 3 mg mL^{-1} bovine fibrinogen (Fg) in PBS, and the concentration of EKCEK–Dox was 0.2 mg mL^{-1}. The samples in different solutions were sealed and put in a constant temperature air shaker (37 °C). Finally, the samples were taken out to check their particle size variation at different time points.

Measurement of drug-loading capacity and drug release of the EKCEK–Dox micelles

Firstly, standard Dox·HCl solutions with different concentrations were prepared and acidized by one drop of concentrated HCl. The absorbance of the solutions was measured by UV spectrophotometer at 485 nm so that the standard UV absorption curve of Dox·HCl was established. 1 mg of EKCEK–Dox was dissolved in 1 mL of acetic acid buffer (pH 3.0) and then shaken in a thermostatic metal bath (50 °C) for 24 h. After that, the above solution was diluted by 9 mL of deionized water acidized by concentrated HCl. At last, the drug-loading capacity (DLC) of EKCEK–Dox could be calculated by the following formula: DLC = (mass of Dox in EKCEK–Dox/mass of EKCEK–Dox) × 100%.

To simulate biosecurity of EKCEK–Dox in blood circulation and the drug release rate in tumor cells, drug release behaviors of EKCEK–Dox in pH 5.0/7.4 buffers were measured respectively. EKCEK–Dox was dialyzed in pH 5.0 and pH 7.4 buffer solutions and shaken in the constant temperature air bath shaker (37 °C). At different time points, a certain amount of dialysate was taken out and acidized by concentrated HCl to check the absorbance of Dox at 485 nm. According to the prefabricated standard UV absorption curve of Dox·HCl, accumulative drug release of EKCEK–Dox in pH 5.0/7.4 buffers could be calculated.

In vitro inhibition efficacy of the EKCEK–Dox micelles on MCF-7 cells

In vitro antitumor efficacy of EKCEK–Dox on MCF-7 cells was measured by MTT assay. MCF-7 cells were cultured by RPMI-1640 medium containing 10% FBS with 5% CO^2 at 37 °C. MCF-7 cells in the logarithmic phase were plated in a 96-well plate by 5×10^3 per well. The EKCEK–Dox micelles were dissolved in RPMI-1640 medium to make the concentration gradient as 1.25 μg mL^{-1}, 2.5 μg mL^{-1}, 5 μg mL^{-1}, 10 μg mL^{-1} and 20 μg mL^{-1} (calculated by Dox). Free Dox and Doxil with corresponding concentrations were dissolved in RPMI-1640 medium and served as positive control groups. Only RPMI-1640 medium without any drugs served as a negative control group. After co-incubated with samples for 12 h, the medium with drugs was removed and replaced by fresh RPMI-1640 medium containing 0.5 μg mL^{-1} MTT. After co-incubated with MTT, the medium was replaced by DMSO solution. Finally, the absorbance of each well was measured by an ELISA reader (MK3, Thermo Co., USA) at 570 nm.

Cellular uptake and endocytosis mechanism of EKCEK–Dox micelles

MCF-7 cells in the logarithmic phase were plated in a 24-well plate by 1×10^5 per well and cultured for 24 h. The RPMI-1640 medium was replaced by fresh medium containing EKCEK–Dox, Doxil and free Dox, and the equivalent concentration of Dox was 8 μg mL^{-1}. After co-incubated with drugs for 2 h and 4 h, the medium containing drugs was removed and corresponding wells were washed by PBS for 2–3 times. Hoechst33342 in PBS was added to stain the cell nucleus for 0.5 h. Finally, the cells were fixed by 4% paraformaldehyde and placed on an inverted fluorescence microscope to observe cellular uptake behavior.

Cellular uptake inhibitors such as chlorpromazine hydrochloride (30 μg mL^{-1}), genistein (15 μg mL^{-1}) and amiloride hydrochloride (133 μg mL^{-1}) were used to inhibit clathrin-mediated endocytosis, caveolin-mediated endocytosis and macropinocytosis, respectively. Before adding the durg-loaded micelles, MCF-7 cells were cultured by RPMI-1640 medium containing different inhibitors for 0.5 h. The fresh medium containing both inhibitors and EKCEK–Dox (10 μg mL^{-1} of equiv. Dox) replaced the above medium, and MCF-7 cells were cultured for another 4 h. Only EKCEK–Dox micelles without inhibitors served as a control group. Eventually, the cells were digested by trypsin and collected, and then the cellular uptake amount of EKCEK–Dox micelles was measured by flow cytometer.

Conclusion

In this study, the doxorubicin-loaded micelles based on zwitterionic oligopeptides EKCEK were successfully fabricated. Since zwitterionic materials have excellent anti-nonspecific protein adsorption property, zwitterionic oligopeptides EKCEK used as drug-loading precursor can make the drug-loaded micelles smoothly circulate in the blood and be nontoxic for the organism. The drug-loading capacity of EKCEK–Dox was up to 44.6%, thus administration dosage can be decreased to some extent. TEM and DLS characterization results showed the mean particle size of the micelles was around 60–80 nm, and size distribution range was very narrow. *In vitro* cell experiment demonstrated the EKCEK–Dox micelles showed much better inhibition efficacy and internalization capacity than Doxil. Therefore, the drug-loaded system based on zwitterionic oligopeptides EKCEK can be a good candidate for delivery of antitumor drugs.

Conflicts of interest

There are no conflicts to declare.

Acknowledgements

The work was supported by the National Natural Science Foundation of China (21674092, 21975216 and 21474085).

References

1 D. Peer, J. M. Karp, S. Hong, O. C. Farokhzad, R. Margalit and R. Langer, *Nat. Nanotechnol.*, 2007, **2**, 751.
2 V. P. Torchilin, *Nat. Rev. Drug Discovery*, 2014, **13**, 813–827.
3 R. Cheng, F. Meng, C. Deng, H.-A. Klok and Z. Zhong, *Biomaterials*, 2013, **34**, 3647–3657.
4 L. Xu, Z. Chu, H. Wang, L. Cai, Z. Tu, H. Liu, C. Zhu, H. Shi, D. Pan and J. Pan, *ACS Appl. Bio Mater.*, 2019, **2**, 3429–3438.
5 Y. C. Barenholz, *J. Controlled Release*, 2012, **160**, 117–134.
6 T. M. Allen and P. R. Cullis, *Adv. Drug Delivery Rev.*, 2013, **65**, 36–48.
7 S. H. Medina, G. Tiruchinapally, M. V. Chevliakov, Y. Y. Durmaz, R. N. Stender, W. D. Ensminger, D. S. Shewach and M. E. ElSayed, *Adv. Healthcare Mater.*, 2013, **2**, 1337–1350.
8 L. M. Kaminskas, V. M. McLeod, B. D. Kelly, C. Cullinane, G. Sberna, M. Williamson, B. J. Boyd, D. J. Owen and C. J. Porter, *Mol. Pharmaceutics*, 2012, **9**, 422–432.
9 H. He, Y. Li, X.-R. Jia, J. Du, X. Ying, W.-L. Lu, J.-N. Lou and Y. Wei, *Biomaterials*, 2011, **32**, 478–487.
10 M. E. Davis, Z. Chen and D. M. Shin, *Nanoscience and technology: a collection of reviews from nature journals*, World Scientific, 2010, pp. 239–250.
11 A. Wicki, D. Witzigmann, V. Balasubramanian and J. Huwyler, *J. Controlled Release*, 2015, **200**, 138–157.
12 V. J. Venditto and F. C. Szoka Jr, *Adv. Drug Delivery Rev.*, 2013, **65**, 80–88.
13 R. K. Jain and T. Stylianopoulos, *Nat. Rev. Clin. Oncol.*, 2010, **7**, 653.
14 H. Cabral and K. Kataoka, *J. Controlled Release*, 2014, **190**, 465–476.
15 Y. Min, J. M. Caster, M. J. Eblan and A. Z. Wang, *Chem. Rev.*, 2015, **115**, 11147–11190.
16 D. E. Discher and A. Eisenberg, *Science*, 2002, **297**, 967–973.
17 J. Gaitzsch, D. Appelhans, L. Wang, G. Battaglia and B. Voit, *Angew. Chem., Int. Ed.*, 2012, **51**, 4448–4451.
18 K. K. Upadhyay, A. N. Bhatt, A. K. Mishra, B. S. Dwarakanath, S. Jain, C. Schatz, J.-F. Le Meins, A. Farooque, G. Chandraiah and A. K. Jain, *Biomaterials*, 2010, **31**, 2882–2892.
19 D. E. Discher, V. Ortiz, G. Srinivas, M. L. Klein, Y. Kim, D. Christian, S. Cai, P. Photos and F. Ahmed, *Prog. Polym. Sci.*, 2007, **32**, 838–857.
20 J. S. Lee and J. Feijen, *J. Controlled Release*, 2012, **161**, 473–483.
21 E. Mabrouk, D. Cuvelier, F. Brochard-Wyart, P. Nassoy and M.-H. Li, *Proc. Natl. Acad. Sci. U. S. A.*, 2009, **106**, 7294–7298.
22 L. Zhao, N. Li, K. Wang, C. Shi, L. Zhang and Y. Luan, *Biomaterials*, 2014, **35**, 1284–1301.
23 L. Xu, V. Selin, A. Zhuk, J. F. Ankner and S. A. Sukhishvili, *ACS Macro Lett.*, 2013, **2**, 865–868.
24 J. D. Robertson, G. Yealland, M. Avila-Olias, L. Chierico, O. Bandmann, S. A. Renshaw and G. Battaglia, *ACS Nano*, 2014, **8**, 4650–4661.
25 Y. Du, W. Chen, M. Zheng, F. Meng and Z. Zhong, *Biomaterials*, 2012, **33**, 7291–7299.
26 H. Sun, F. Meng, R. Cheng, C. Deng and Z. Zhong, *Acta Biomater.*, 2014, **10**, 2159–2168.
27 T. Thambi, V. Deepagan, H. Ko, D. S. Lee and J. H. Park, *J. Mater. Chem.*, 2012, **22**, 22028–22036.
28 F. Liu, V. Kozlovskaya, S. Medipelli, B. Xue, F. Ahmad, M. Saeed, D. Cropek and E. Kharlampieva, *Chem. Mater.*, 2015, **27**, 7945–7956.
29 C.-Y. Chen, T. H. Kim, W.-C. Wu, C.-M. Huang, H. Wei, C. W. Mount, Y. Tian, S.-H. Jang, S. H. Pun and A. K.-Y. Jen, *Biomaterials*, 2013, **34**, 4501–4509.
30 L. Xu, H. Wang, Z. Chu, L. Cai, H. Shi, C. Zhu, D. Pan, J. Pan, X. Fei and Y. Lei, *ACS Appl. Polym. Mater.*, 2020, **2**, 741–750.
31 Y. Lu, A. Zhuk, L. Xu, X. Liang, E. Kharlampieva and S. A. Sukhishvili, *Soft Matter*, 2013, **9**, 5464–5472.
32 J. V. Georgieva, R. P. Brinkhuis, K. Stojanov, C. A. Weijers, H. Zuilhof, F. P. Rutjes, D. Hoekstra, J. C. van Hest and I. S. Zuhorn, *Angew. Chem., Int. Ed.*, 2012, **51**, 8339–8342.
33 H. Gao, S. Zhang, S. Cao, Z. Yang, Z. Pang and X. Jiang, *Mol. Pharmaceutics*, 2014, **11**, 2755–2763.
34 L. Pourtau, H. Oliveira, J. Thevenot, Y. Wan, A. R. Brisson, O. Sandre, S. Miraux, E. Thiaudiere and S. Lecommandoux, *Adv. Healthcare Mater.*, 2013, **2**, 1420–1424.
35 B. Zhang, S. Wan, X. Peng, M. Zhao, S. Li, Y. Pu and B. He, *J. Mater. Chem. B*, 2020, **8**, 3939–3948.
36 G. Ma, W. Lin, Z. Wang, J. Zhang, H. Qian, L. Xu, Z. Yuan and S. Chen, *J. Mater. Chem. B*, 2016, **4**, 5256–5264.
37 G. Ma, W. Lin, Z. Yuan, J. Wu, H. Qian, L. Xu and S. Chen, *J. Mater. Chem. B*, 2017, **5**, 935–943.
38 Z. Wang, G. Ma, J. Zhang, Z. Yuan, L. Wang, M. Bernards and S. Chen, *Biomaterials*, 2015, **62**, 116–127.
39 S. Chen, J. Zheng, L. Li and S. Jiang, *J. Am. Chem. Soc.*, 2005, **127**, 14473–14478.
40 M. O. Oyewumi, R. A. Yokel, M. Jay, T. Coakley and R. J. Mumper, *J. Controlled Release*, 2004, **95**, 613–626.

